Available online at www.sciencedirect.com

ScienceDirect

IFAC Papers Online CONFERENCE PAPER ARCHIVE

IFAC-PapersOnLine 48-30 (2015) 282–287

Comprehensive Modelling and Small Signal Stability Analysis of RES-based Microgrid

Awan Krismanto* N. Mithulananthan ** *Kwang Y. Lee* ***

**School of ITEE, University of Queensland, Brisbane, Australia (e-mail: a.krismanto@ uq.edu.au), Department of Electrical Engineering, Institut Teknologi Nasional, Malang, Indonesia*
*** School of ITEE, University of Queensland, Brisbane, Australia (e-mail: mihtulan@ itee.uq.edu.au)*
**** Department of Electrical & Computer Engineering, Baylor University,Baylor (e-mail: Kwang_Y_Lee@baylor.edu)*

Abstract: Implementation of power electronic devices has introduced novel challenges in microgrid (MG) operation and control; and hence the condition of power electronic devices should be monitored for stable operation of the entire grid. This paper presents detailed small signal model of the MG based upon Renewable Energy Resources (RESs), focusing on the dynamic behavior of power electronic devices and associated controllers. Variations on inverter modulation indices and boost converter duty cycles were applied to observe small signal stability performance of the MG. Eigenvalues and participation factor analysis were presented to identify weak modes and stability margin. Analysis of eigenvalue loci shows motion of low frequency loci toward the right-half complex plane as the parameters of power electronic devices varied. More severe oscillatory behavior was experienced when fluctuation occurred at the grid-side inverter, which indicates fast degradation of damping and stability margin. The presented work contributes to help utilities in designing a stable MG for seamless integration of renewable energy into power systems.

Keywords: Microgrid, small signal stability, inverter, duty cycle, modulation index, renewable energy sources.

1. INTRODUCTION

Distributed generations (DGs) based on renewable energy resources (RESs) have offered viable solution for remote area electrification. Moreover, increase of local loads with DGs in distribution system has lead to a configuration of small-scale power system called microgrid (MG). The MG has been defined as a system with distributed energy resources, equipped by energy storage system (ESS) and associated load with both grid-connected and islanding operation capabilities. In the grid-connected mode of operation, most of the power demand is supplied by the main grid, hence a constant power output from MG should be maintained. During the islanding or autonomous mode of operation, DGs and energy storage systems must keep the local voltage and frequency stable. Power fluctuations in MGs, furthermore, contribute to the voltage and frequency stability degradation of the entire system. Except for large disturbances, power fluctuation in MG can be regarded as small signal stability problem (Majumder, 2013).

Power electronic devices have played an important role to admit the fluctuating characteristics of MG. A typical MG system has incorporated power electronic devices as interfacing equipment to meet grid voltage and frequency requirements (Justo et al., 2013). Recent development of PV technologies has encouraged integration of DC/DC step-up converter and DC/AC inverter within the system. DC/AC inverter has been appropriate for fuel cell and ESS. Since then, back-to-back inverter system has improved performance of the wind energy conversion system (WECS). In the DC-MG architecture, DC/DC step-up converter has been embedded to PV, fuel cell and ESS. Whereas, AC/DC conversion system has been applied to WECS to produce controllable DC voltage. Implementation of power electronic devices, however, has introduced some challenges in MG operation and control. Power electronic devices are complex active systems which are sensitive to oscillations resulting from network disturbances because of their negligible physical inertia (Pogaku, Prodanovic, and Green, 2007). Fluctuating energy sources presuppose adjustment in the control scheme of switching equipment, and hence, the modulation indices and duty cycle of power electronics devices will be fluctuating as well.

It is necessary to establish the stability boundary of the DG interfacing system in order to ensure proper operation and acceptable stability performance of the grid (Kroutikova, Hernandez-Aramburo, and Green, 2007). Full order models of DGs and coupling devices are required to obtain complete picture, especially for small signal stability concern (Tang, Deng and Qi, 2014). To date, however, there are lack of MG models involving dynamic switching action and common PWM control system associated with power electronic devices in small signal stability analysis. Presenting power electronic devices as ideal voltage sources in stability investigation carried incomplete analysis since it would not contribute to dynamic stability of the system (Katiraei, Iravani, and Lehn, 2007; Nimpitiwan and Kaitwanidvilai, 2012; Kroutikova, Hernandez-Aramburo, and Green, 2007).

A small signal stability analysis in a typical AC-MG consisting of PV, WECS and salient pole synchronous generator is

10.1016/j.ifacol.2015.12.391

addressed in this paper. The analysis emphasizes on power electronic dynamics in inverting, rectifying and boosting operations. Duty cycle and modulation indices which indicate the ability of control scheme of the converter to deliver power are varied. Stability margin of the open-loop system afterward will be identified through participation factor and eigenvalue trajectories analysis.

2. MODEL OF MICROGRID COMPONENTS

Typical model of AC-MGs analysed in this paper consists of three DGs; WECS, PV and diesel engine generator as shown in Fig. 1.

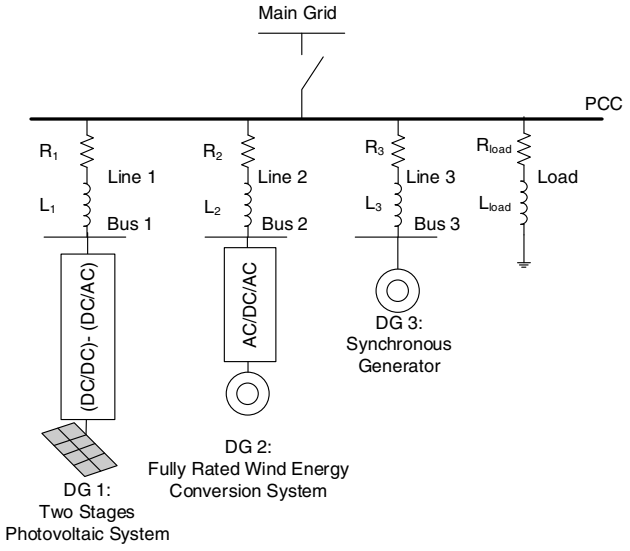

Fig. 1. AC Microgrid Model.

Power electronic devices have become substantial parts in MG topologies. PV system is equipped with two stages of converters. The DC/DC boost converter adjusts fluctuating DC voltage from solar array panels into a desired DC voltage level and DC/AC inverter then converts the DC voltage into a specified AC voltage. The WECS incorporates a back-to-back AC/DC/AC converter to obtain regulated AC voltage with desired magnitude and frequency.

Averaged and linearized state-space models with variation on modulation indices and duty cycle will be derived for small signal stability studies. State-space models of the components in the entire system are represented on their individual reference frame hence all DG units need to be aligned into the common reference frame using transformation technique presented in (Pogaku, Prodanovic, and Green, 2007). Output current and input bus voltage of DG units in common reference frame are presented as

$$\begin{bmatrix}\Delta i_{oDi}\\ \Delta i_{oQi}\end{bmatrix} = T_c\begin{bmatrix}\Delta i_{odi}\\ \Delta i_{oqi}\end{bmatrix} + T_{c\delta}\left[\Delta\delta_i\right] \tag{1}$$

$$\begin{bmatrix}\Delta v_{bdi}\\ \Delta v_{bqi}\end{bmatrix} = T_v\begin{bmatrix}\Delta v_{bDi}\\ \Delta v_{bQi}\end{bmatrix} + T_{v\delta}\left[\Delta\delta_i\right] \tag{2}$$

$$T_c = \begin{bmatrix}\cos(\delta_{0i}) & -\sin(\delta_{0i})\\ \sin(\delta_{0i}) & \cos(\delta_{0i})\end{bmatrix}, T_{c\delta} = \begin{bmatrix}-I_{0d}\sin(\delta_0) - I_{0q}\cos(\delta_0)\\ I_{0d}\cos(\delta_0) - I_{0q}\sin(\delta_0)\end{bmatrix}$$

$$T_v = \begin{bmatrix}\cos(\delta_{0i}) & \sin(\delta_{0i})\\ -\sin(\delta_{0i}) & \cos(\delta_{0i})\end{bmatrix}, T_{v\delta} = \begin{bmatrix}-V_{bD0}\sin(\delta_0) + V_{bQ0}\cos(\delta_0)\\ -V_{bD0}\cos(\delta_0) - V_{bQ0}\sin(\delta_0)\end{bmatrix}$$

where $\delta_i$refer to the phase angle of individual DGs respect to their reference frames and

2.1 State-Space Model of DC/DC Step-Up Converter

The DC-DC boost converter has two stages of operation modes over one period. Duty cycle (d) denotes time range when the power electronic switch is *on.* Inductor input current (i_b), inductor output current (i_{dc}), and capacitor voltage (v_{dc}) are chosen as state variables. Input DC voltage (v_g) is dictated as input variable. Complete model of DC/DC boost converter is obtained through the averaged technique in (Erickson and Maksimovic, 2001) given by

$$\begin{bmatrix}\Delta\dot{i}_b\\ \Delta\dot{i}_s\\ \Delta\dot{v}_{dc}\end{bmatrix} = \begin{bmatrix}-\frac{(1-d)R_{cb}+R_b}{L_b} & \frac{(1-d)R_{cb}}{L_b} & -\frac{(1-d)}{L_b}\\ \frac{(1-d)R_{cb}}{L_s} & -\frac{(1-2d)R_{cb}+R_s}{L_s} & \frac{1}{L_s}\\ \frac{(1-d)}{C_{dc}} & -\frac{1}{C_{dc}} & 0\end{bmatrix}\begin{bmatrix}\Delta i_b\\ \Delta i_s\\ \Delta v_{dc}\end{bmatrix} + \begin{bmatrix}\frac{1}{L_b}\\ 0\\ 0\end{bmatrix}\left[\Delta v_g\right] \tag{3}$$

2.2 State-Space Model of DC/AC Converter

For small signal stability analysis, only low frequency model of inverter is considered, assuming that high frequency components are attenuated by interface low pass filter (Nimpitiwan and Kaitwanidvilai, 2012). Dynamic operation of PWM control can be approximated into discrete switching function corresponding to the duty cycle and modulation indices (Abdel-Rahim and Quaicoe, 1996). State variables of inverter system consist of DC side current (i_s), DC side voltage (v_d), VSI current (i_{ivd}, i_{ivq}), coupling inductor current (i_{oq}, i_{od}), and capacitor voltage in the interface low pass filter (v_{od}, v_{oq}) as presented in (Abdel-Rahim and Quaicoe, 1996) is given by

$$\begin{bmatrix}\Delta\dot{i}_s\\ \Delta\dot{v}_s\\ \Delta\dot{i}_{ivd}\\ \Delta\dot{i}_{ivq}\\ \Delta\dot{v}_{od}\\ \Delta\dot{v}_{oq}\\ \Delta\dot{i}_{od}\\ \Delta\dot{i}_{oq}\end{bmatrix} = \begin{bmatrix}-\frac{R_s}{L_s} & -\frac{1}{L_s} & 0 & 0 & 0 & 0 & 0 & 0\\ \frac{1}{C_d} & 0 & -\frac{m_{di}\sqrt{3}}{4C_d} & -\frac{m_{qi}\sqrt{3}}{4C_d} & 0 & 0 & 0 & 0\\ 0 & \frac{m_{di}\sqrt{3}}{4L_f} & -\frac{R_f}{L_f} & -\omega & -\frac{1}{L_f} & 0 & 0 & 0\\ 0 & \frac{m_{qi}\sqrt{3}}{4L_f} & \omega & -\frac{R_f}{L_f} & 0 & -\frac{1}{L_f} & 0 & 0\\ 0 & 0 & \frac{1}{C_f} & 0 & 0 & -\omega & -\frac{1}{C_f} & 0\\ 0 & 0 & 0 & \frac{1}{C_f} & \omega & 0 & 0 & -\frac{1}{C_f}\\ 0 & 0 & 0 & 0 & \frac{1}{L_c} & 0 & -\frac{R_c}{L_c} & -\omega\\ 0 & 0 & 0 & 0 & 0 & \frac{1}{L_c} & \omega & -\frac{R_c}{L_c}\end{bmatrix}\begin{bmatrix}\Delta i_s\\ \Delta v_s\\ \Delta i_{ivd}\\ \Delta i_{ivq}\\ \Delta v_{od}\\ \Delta v_{oq}\\ \Delta i_{od}\\ \Delta i_{oq}\end{bmatrix} + \begin{bmatrix}\frac{1}{L_c}\\ 0\\ 0\\ 0\\ 0\\ 0\\ 0\\ 0\end{bmatrix}\left[\Delta v_{dc}\right] \tag{4}$$

where m_{di} and m_{qi} are modulation indices of VSI.

2.3 State Space Model of AC/DC Converter

State variables of rectifier consist of AC side current (i_{rd}, i_{rq}) and DC side voltage (v_{dcout}). General state-space model of AC/DC rectifier in the rotating frame reference by ignoring zero sequence component (Wu et al., 1990), is given below.

$$\begin{bmatrix} \Delta\dot{i}_{rd} \\ \Delta\dot{i}_{rq} \\ \Delta\dot{v}_{dcout} \end{bmatrix} = \begin{bmatrix} -\frac{R_S}{L_S} & -\omega & -\frac{m_r\sqrt{3}}{4L_S} \\ \omega & -\frac{R_S}{L_S} & -\frac{m_r\sqrt{3}}{4L_S} \\ \frac{m_r\sqrt{3}}{4C_{out}} & \frac{m_r\sqrt{3}}{4C_{out}} & 0 \end{bmatrix} \begin{bmatrix} \Delta i_{rd} \\ \Delta i_{rq} \\ \Delta v_{dcout} \end{bmatrix} + \begin{bmatrix} 1 & 0 & 0 \\ 0 & 1 & 0 \\ 0 & 0 & -\frac{1}{C_{out}} \end{bmatrix} \begin{bmatrix} \Delta e_d \\ \Delta e_q \\ \Delta i_S \end{bmatrix} \quad (5)$$

where m_r is the modulation index of the rectifier.

2.4 State-Space Model of Lines and Load

There are three line impedances which connected each DG with the point of common connection (PCC). Moreover, all of DG units supplied a central load, through the single PCC bus. Linearized state-space model for line (i_{liDk}, i_{liQk}) and load (i_{loD}, i_{loQ}) currents in the common reference frame is given by

$$\begin{aligned} \Delta\dot{x}_{lik} &= A_{lik}\Delta x_{lik} + B_{lik}\Delta v_{bkDQ} + B_{lo}\Delta v_{pccDQ} \\ \Delta x_{lik} &= \begin{bmatrix} \Delta i_{linekDQ} \end{bmatrix}^T, \Delta v_{bkDQ} = \begin{bmatrix} \Delta v_{bkD} & \Delta v_{bkQ} \end{bmatrix}^T \\ \Delta v_{pccDQ} &= \begin{bmatrix} \Delta v_{pccD} & \Delta v_{pccQ} \end{bmatrix}^T \end{aligned} \quad (6)$$

where *k* indicates the DG bus number. State equation of lines and a central load are given by

$$\begin{aligned} \Delta\dot{x}_{line} &= A_{line}\Delta x_{line} + B_{line}\Delta v_{bline} + B_{lo}\Delta v_{pccDQ} \\ \Delta x_{line} &= \begin{bmatrix} \Delta i_{line1DQ} & \Delta i_{line2DQ} & \Delta i_{line3DQ} \end{bmatrix}^T \\ \Delta v_{bline} &= \begin{bmatrix} \Delta v_{b1DQ} & \Delta v_{b2DQ} & \Delta v_{b3DQ} \end{bmatrix}^T \end{aligned} \quad (7)$$

$$\Delta\dot{x}_{lo} = A_{lo}\Delta x_{lo} + B_{lo}\Delta v_{pccDQ}, \Delta x_{lo} = \begin{bmatrix} \Delta i_{oD} & \Delta i_{oQ} \end{bmatrix}^T \quad (8)$$

State matrices of line and load currents in the previous equations are presented as A_{line} and A_{lo} respectively. Estimation of bus voltages is then obtained by assuming implementation of virtual resistance (R_N) as presented in (Pogaku Prodanovic, M. & Green, 2007).

3. MICROGRID STATE-SPACE MODEL

3.1 State-Space Model of Two Stage PV System

State-space model for two stage PV conversion system composed of DC/DC boost converter and DC/AC inverter is presented by (3) to (4). Linearized small signal model of the two stage PV system is

$$\begin{aligned} \Delta\dot{x}_{pv} &= A_{pv}\Delta x_{pv} + B_{pv}\Delta u_{pv} + B_{vpv}\Delta v_{b1dq} \\ \Delta i_{odq} &= \begin{bmatrix} 0_{2\times 8} & I_{2\times 2} \end{bmatrix}\Delta x_{pv} \\ \Delta x_{pv} &= \begin{bmatrix} \Delta i_b & \Delta i_s & \Delta v_b & \Delta v_d & \Delta i_{ivd1} & \Delta i_{ivq1} & \Delta v_{od1} & \Delta v_{oq1} \\ & \Delta i_{od1} & \Delta i_{oq1} \end{bmatrix}^T \end{aligned} \quad (9)$$

$$\Delta u_{pv} = \begin{bmatrix} \Delta v_{gpv} & \Delta\delta_1 \end{bmatrix}^T, \Delta v_{b1} = \begin{bmatrix} \Delta v_{b1d} & \Delta v_{b1q} \end{bmatrix}^T$$

Output current of PV system has to be translated into the common reference frame according to (1) as given by

$$\begin{bmatrix} \Delta i_{oDQ\_pv} \end{bmatrix} = C_{pv}\begin{bmatrix} \Delta x_{pv} \end{bmatrix} + T_{c\delta}\begin{bmatrix} \Delta\delta_{pv} \end{bmatrix}, C_{pv} = \begin{bmatrix} 0_{2\times 8} & T_c \end{bmatrix} \quad (10)$$

Reverse transformation into an individual reference frame for the bus voltage is needed. This transformation procedure can be conducted by implementing (2) in (9). Equation of input bus voltage in PV system is obtained as

$$\begin{aligned} \begin{bmatrix} \Delta v_{b1dq} \end{bmatrix} &= B_{pvb}\begin{bmatrix} \Delta x_{pv} \end{bmatrix} + B_{pvl}\begin{bmatrix} \Delta i_{line1DQ} \end{bmatrix} + B_{\delta pv}\begin{bmatrix} \Delta\delta_{pv} \end{bmatrix} \\ B_{pvb} &= R_N B_{vpv} T_v C_{pv}, \quad B_{pvl} = R_N B_{vpv} T_v, \\ B_{\delta pv} &= B_{vpv}\left(T_v R_N T_{c\delta} + T_{v\delta}\right) \end{aligned} \quad (11)$$

where L_c is coupling inductance between PV system and local bus. δ_1 is phase angle deviation of the PV system respect to the common reference frame.

3.2 State-Space Model of Fully Rated WECS System

Fully rated converter model for WECS mainly consist of wind turbine, induction generator and inverter system. This configuration has some advantages regarding the capability of variable speed operation and additional isolation of inverter system (Ugalde-Loo and Ekanayake, 2013). AC/DC/AC model can be obtained from integration of (4) and (5).

Induction generator model presented in this paper is adopted from (Krause Wasynczuk, and Sudhoff, 2002; Ugalde-Loo and Ekanayake, 2013). Stator and rotor currents in rotating frame reference $(i_{sd}, i_{sq}, i_{rd}, i_{rq})$ become state variables while input variables are stator (v_{sd}, v_{sq}), rotor (v_{rd}, v_{rq}) and bus 2 voltages (v_{b2d}, v_{b2q}). The model is completed by mechanical equations of wind turbine and electromagnetic torque, respectively, as

$$\frac{d\omega_r}{dt} = \frac{1}{2H}\left(T_m - T_e\right) \quad (12)$$

$$T_e = X_m\left(i_{qs}i_{dr} - i_{ds}i_{qr}\right) \quad (13)$$

State-space equation for fully rated converter WECS is derived from combination of equations (4), (5), (12) and (13). Linearized state space equations of WECS are presented as

$$\begin{aligned} \Delta\dot{x}_W &= A_W\Delta x_W + B_W\Delta u_W + B_{vW}\Delta v_{b2} \\ \Delta i_{odq} &= \begin{bmatrix} 0_{2\times 14} & I_{2\times 2} \end{bmatrix}\Delta x_W \end{aligned} \quad (14)$$

$$\begin{aligned} \Delta x_w = \begin{bmatrix} \Delta i_{sd2} & \Delta i_{sq2} & \Delta i_{rd2} & \Delta i_{rq2} & \Delta\omega_{r2} & \Delta i_{dr2} & \Delta i_{qr2} & \Delta v_{dcout} \\ \Delta i_{s2} & \Delta v_{d2} & \Delta i_{ivd2} & \Delta i_{ivq2} & \Delta v_{cd2} & \Delta v_{cq2} & \Delta i_{od2} & \Delta i_{oq2} \end{bmatrix}^T \\ \Delta u_w = \begin{bmatrix} \Delta v_{sd2} & \Delta v_{sq2} & \Delta v_{rd2} & \Delta v_{rq2} & \Delta T_{mw} & \Delta\delta_w \end{bmatrix}^T \\ \Delta v_{b2} = \begin{bmatrix} \Delta v_{bd2} & \Delta v_{bq2} \end{bmatrix}^T \end{aligned}$$

Current output and voltage input equations of WECS after synchronization process are determined as

$$\begin{bmatrix} \Delta i_{oDQ\_w} \end{bmatrix} = C_w\begin{bmatrix} \Delta x_w \end{bmatrix} + T_{c\delta}\begin{bmatrix} \Delta\delta_w \end{bmatrix}, C_w = \begin{bmatrix} 0_{2\times 14} & T_c \end{bmatrix} \quad (15)$$

$$\left[\Delta v_{vb2dq}\right] = B_{wb}\left[\Delta x_w\right] + B_{wl}\left[\Delta i_{line2DQ}\right] + B_{\delta w}\left[\Delta\delta_2\right]$$
$$B_{wb} = R_N B_{vw} T_v C_w,\ B_{wl} = R_N B_{vw} T_v,\ B_{\delta w} = B_{vw}\left(T_v R_N T_{c\delta} + T_{v\delta}\right) \quad (16)$$

δ_2 is the phase angle deviation of WECS system respected to common reference frame.

3.3 Diesel Engine Generator System

Synchronous generator in diesel DG unit is presented in the form of non-reduced order involving dynamics at stator, rotor and damper winding. Rotor is modelled as two q axis (i_{kq1}, i_{kq2}) and one d axis (i_{kd}) currents, while stator is modelled as one q axis (i_{qs}) and one d axis (i_{ds}) current. Rotor excitation can be stated as generator field current (i_{fd}). Input of state-space model are stator (v_{ds}, v_{qs}) and field winding voltage (v_{fd}). Output variables are stator current (i_{ds}, i_{qs}). Electromagnetic torque is expressed by

$$T_e = \left(X_{sq} - X_{sd}\right) i_{sd} i_{sq} + X_{md}\left(i_{fd} + i_{kd}\right) i_{sq} - X_{mq}\left(i_{kq1} + i_{kq2}\right) i_{sd} \quad (17)$$

Synchronous machine unit is determined as the common reference frame. Reference frequency for MG system is provided by these units, hence equations which reveal relationship between frequency deviation and rotor angle in synchronous generator should be involved in the state variable. State-space equation of this DG unit is completed by connecting diesel unit to local bus 3. Linearized state equation of synchronous machine derived from (Krause, Wasynczuk, and Sudhoff, 2002, Ugalde-Loo and Ekanayake, 2013) is presented as

$$\Delta\dot{x}_d = A_d \Delta x_d + B_{vd} \Delta u_d$$
$$\begin{bmatrix} \Delta i_{odq} \\ \Delta\delta \end{bmatrix} = \begin{bmatrix} I_{2\times2} & 0_{2\times5} & 0 \\ 0 & 0_{1\times5} & 1 \end{bmatrix} \Delta x_d \quad (18)$$

$$\Delta x_d = \begin{bmatrix} \Delta i_{sd} & \Delta i_{sq} & \Delta i_{fd} & \Delta i_{kd} & \Delta i_{kq1} & \Delta i_{kq2} & \Delta\omega_r & \Delta\delta \end{bmatrix}^T$$
$$\Delta u_d = \begin{bmatrix} \Delta v_{bd3} & \Delta v_{bq3} & \Delta v_{fd3} & \Delta T_m \end{bmatrix}^T$$

Since diesel unit is operated as reference, translation of output and input variables in this DG unit is not necessary. Equation related to output current and input bus voltage for diesel are given by

$$\left[\Delta i_{oDQ\_d}\right] = C_d\left[\Delta x_d\right]$$
$$\left[\Delta v_{b3dq}\right] = B_{db}\left[\Delta x_d\right] + B_{dl}\left[\Delta i_{line3DQ}\right]$$
$$B_{db} = R_N B_{vd} C_d,\ B_{dl} = R_N B_{vd} \quad (19)$$

3.4 Connection between Lines and DG Units

Relationship between lines and DG units are provided by bus voltages. From (6), bus voltages are obtained from multiplication of aligned output currents from DG units and the virtual resistance as given by

$$\Delta\dot{x}_{li1} = A_{li1}\Delta x_{li1} + B_{li\_pv}\Delta x_{pv},\ B_{li\_pv} = R_N C_{pv}$$
$$\Delta\dot{x}_{li2} = A_{li2}\Delta x_{li2} + B_{li\_w}\Delta x_w,\ B_{li\_w} = R_N C_w$$
$$\Delta\dot{x}_{li3} = A_{li3}\Delta x_{li3} + B_{li\_d}\Delta x_d,\ B_{li\_d} = R_N C_d \quad (20)$$

3.5 Connection between Lines and Central Load

Substitution of input bus and PCC voltage with lines and loads currents in (6), (7) and (8) yield the complete line and load state equations as given by

$$\Delta\dot{x}_{line} = A_{line}\Delta x_{line} + B_{li}\Delta i_{lineDQ} + B_{li-lo}\,\Delta i_{oDQ}$$
$$B_{li} = R_N B_{lik},\ B_{li\_lo} = R_N B_{li\_lok} \quad (21)$$

$$\Delta\dot{x}_{lo} = A_{load}\Delta x_{lo} + B_{lo}\Delta i_{loadDQ} + B_{lo-li}\,\Delta i_{lineDQ}$$
$$B_{lo} = R_N B_{lok},\ B_{lo\_li} = R_N B_{lo\_lik} \quad (22)$$

3.6 Complete Model of Microgrid

Complete linearized state-space model of MG system consists of PV, WECS and synchronous generator involving connection among DG units, network and central load. State equation of these model is presented as

$$\Delta\dot{x}_{MG} = A_{MG}\Delta x_{MG} + B_{MG}\Delta u_{MG} + B_{v1MG}\Delta v_b + B_{v2MG}\Delta v_{pcc}$$
$$\Delta x_{MG} = \begin{bmatrix} \Delta x_{pv} & \Delta x_w & \Delta x_d & \Delta x_{net} & \Delta x_{load} \end{bmatrix}^T$$
$$\Delta u_{MG} = \begin{bmatrix} \Delta v_{gpv} & \Delta v_{sdw} & \Delta v_{sqw} & \Delta v_{rdw} & \Delta v_{rqw} & \Delta T_{mw} & \Delta v_{fd3} & \Delta T_{md} \end{bmatrix}^T$$
$$A_{MG} = \begin{bmatrix} A_{pv} + B_{pvb} & 0 & B_{\delta pv} & B_{pvl} & 0 \\ 0 & A_w + B_{wb} & B_{\delta w} & B_{wl} & 0 \\ 0 & 0 & A_d + B_{db} & B_{dl} & 0 \\ B_{li\_pv} & B_{li\_w} & B_{li\_d} & A_{li} + B_{li} & B_{li\_lo} \\ 0 & 0 & 0 & B_{lo\_li} & A_{lo} + B_{lo} \end{bmatrix} \quad (23)$$

4. SIMULATION RESULT

The AC-MG system consisting of PV, WECS and synchronous generator was investigated. Each DG's local bus were connected to PCC bus through appropriate line impedance. A specific central load was connected to the PCC bus. Wind induction generator and salient pole synchronous generator parameters were adopted from (Ugalde-Loo et al., 2013; Ugalde-Loo and Ekanayake, 2010).

Variation on control parameters of power electronics devices were applied to analyze small signal stability performance of the MG. PV system duty cycle (d) and modulation indices (m_{pv}). WECS modulation indices both in generator and grid side inverter (m_{w1}, m_{w2}) were varied to investigate contribution of fluctuated condition of power electronic devices to dynamics stability performance in MG system. Participation factor and trajectory analysis of eigenvalues were then conducted to obtain important information relating to system behaviour and response when it was subjected to small parameter variations.

Investigated MG model had 42 modes, with all loci of eigenvalues located at open left-half plane as shown in Fig. 2. This indicated that MG system was stable around its operating point. Participation factors of these eigenvalues were considered to investigate sensitivity of different state variables during selected parameter variations. This analysis showed that synchronous generator stator currents and load currents participated more to modes in cluster 1 while output currents

Table 1. Participation Factors of Low Frequency Eigenvalues.

Modes $\lambda_{14,15}$		Modes $\lambda_{16,17}$		Modes $\lambda_{18,19}$		Modes $\lambda_{20,21}$		Modes $\lambda_{22,23}$		Modes $\lambda_{24,25}$		Modes $\lambda_{26,27}$	
State	P	State	P	State	P	State	P	State	P	State	P	State	P
v_{d_PV}	0.018	v_{d_PV}	0.009	v_{d_PV}	0.221	v_{d_PV}	0.301	v_{d_w}	0.392	v_{d_w}	0.099	v_{d_w}	0.008
i_{invd_PV}	0.249	i_{invd_PV}	0.249	i_{invd_PV}	0.002	i_{invd_PV}	0.001	i_{invd_w}	0.081	i_{invd_w}	0.198	i_{invd_w}	0.223
i_{invq_PV}	0.249	i_{invq_PV}	0.249	i_{invq_PV}	0.002	i_{invq_PV}	0.001	i_{invq_w}	0.081	i_{invq_w}	0.198	i_{invq_w}	0.223
v_{od_PV}	0.241	v_{od_PV}	0.245	v_{od_PV}	0.008	v_{od_PV}	0.007	v_{od_w}	0.024	v_{od_w}	0.213	v_{od_w}	0.240
v_{oq_PV}	0.241	v_{oq_PV}	0.245	v_{oq_PV}	0.008	v_{oq_PV}	0.007	v_{oq_w}	0.024	v_{oq_w}	0.213	v_{oq_w}	0.240
i_{s_PV}	0.000	i_{s_PV}	0.000	i_{s_PV}	0.488	i_{s_PV}	0.430	i_{s_w}	0.280	i_{s_w}	0.121	i_{s_w}	0.067

P: participation factor

from PV and WECS associated with modes in cluster 2. Eigenvalues in both clusters 1 and 2 were highly damped and did not contribute to small signal stability of the MG system. Angular frequency, stator and rotor current of WECS associated with high frequency of modes on cluster 3. All of the aforementioned groups of eigenvalues were asymptotically stable, indicated by their relative fixed positions during small variation on power electronic devices control parameters. Low frequency component of eigenvalues in cluster 4 were very sensitive when system was exposed to small fluctuation on power electronic devices parameters in PV and WECS system.

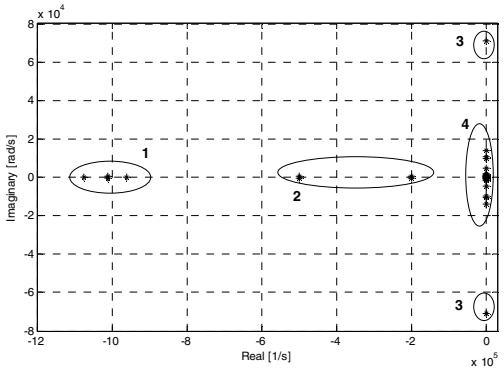

Fig. 2. Microgrid eigenvalues in steady state condition.

Modulation indices and duty cycle of power electronic devices varied in accordance to different input power of the DG units. Circumstances related to the variation of these parameters would impact MG operation especially on the islanding mode. Specifically, this would cause dynamic condition in DC link of inverter system and output state variables of the DG unit which would influence system stability. DC link and output voltage of DG units should be maintained at specified limits through power electronics controller, to prevent instability. Table 1 showed participation factors analysis result which indicated connection between state variables and the modes due to variation on the power electronic devices parameters.

Fig. 3 showed trajectories of eigenvalues in the MG due to small variation on PV system duty cycles of DC/DC boost converter. As duty cycle decreased from 0.75 to 0.3, trajectory analysis of modes $\lambda_{18,19}$ and $\lambda_{20,21}$ showed right shift movement toward open right-half plane. It could be noted that DC link current and voltage of PV system which participated dominantly in modes $\lambda_{18,19}$ and $\lambda_{20,21}$ were highly sensitive due to duty cycle variation.

Trajectories of eigenvalues during modulation indices variation in PV system DC/AC inverter is depicted in Fig. 4 consisted of medium frequency and low frequency oscillation modes. Loci of eigenvalues became more sensitive than in previous fluctuation. It can be seen that two of four pairs loci eigenvalues, i.e., $\lambda_{18,19}$ and $\lambda_{20,21}$ shifted toward the right of imaginary axis while the other pairs of $\lambda_{14,15}$ and $\lambda_{16,17}$ moved toward left as modulation indices decreased from 0.785 to 0.3. Medium frequency oscillation modes, marked with $\lambda_{14,15}$ and $\lambda_{16,17}$, shifted toward left side of open left-half plane. This revealed that during modulation indices fluctuation, inverter current and output voltage in PV system became more stable. Low frequency modes however, experienced degradation of stability limits during these variations. DC link current and voltage which referred to modes $\lambda_{18,19}$ and $\lambda_{20,21}$ moved toward open right half plane. Extensive motion of $\lambda_{18,19}$ to zero axis implied rapid deterioration of damping and increased of oscillations would occur in low frequency region. Furthermore, this eventually tended to instability.

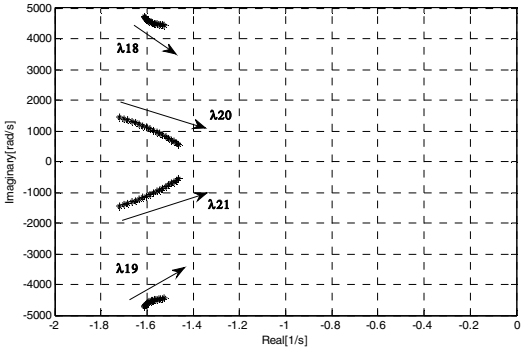

Fig. 3. Low frequency eigenvalues in PV duty cycle variation.

Loci eigenvalues shifting due to variation on control parameters of power electronic devices in WECS was system depicted in Fig. 5. As modulation indices of grid-side DC/AC inverter in WECS was varied from 0.785 to 0.3, both DC side and AC side of WECS were impacted. Improvement of stability boundary were experienced by inverter current and output voltage in modes $\lambda_{24,25}$ and $\lambda_{26,27}$, indicated by left shift movement of the eigenvalues. On the other hand, DC link voltage and current between AC/DC and DC/AC in WECS faced fast stability degradation. It was represented by extensive right movement of modes $\lambda_{22,23}$. This might result in more oscillatory condition in DC link current and voltage. However, when dealing with variation on induction generator side AC/DC rectifier, eigenvalues $\lambda_{22,23}$, $\lambda_{24,25}$, and $\lambda_{26,27}$ were relatively remaining in their idle position. It could be

noted that small deviation on this rectifier circuit would not contribute significantly to the MG's small signal stability.

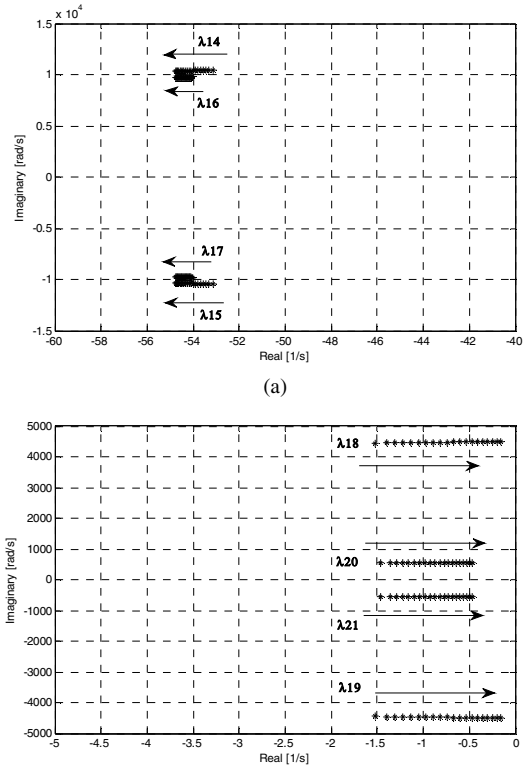

Fig. 4. Microgrid eigenvalues in DC/AC PV system modulation indices variation at (a) medium, (b) low frequency modes.

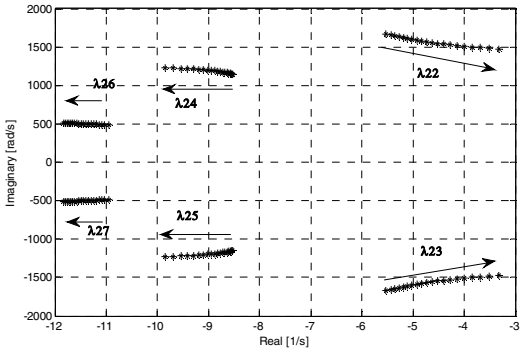

Fig. 5. Low frequency eigenvalues in WECS modulation indices variation in the grid-side converter.

5. CONCLUSIONS

A detailed small signal model of RESs based MG focused on dynamic behaviour of power electronics devices is presented. Small signal stability analysis is conducted to investigate damping and stability limits during applied small fluctuation on inverter duty cycle and modulation indices. Eigenvalues and participation factor analysis are then carried out to recognize weak modes of MG system. The simulation results reveal new concern on small signal stability in the MG. It is monitored that variation of control parameters of power electronic devices causes fast damping degradation of DC link and output variables of DG units. Furthermore it can lead to instability when variation occurred in the grid-side inverter. This should be considered to provide reliable control system ensuring stable operation of MG. This paper provides general theoretical approach on the influence of power electronic devices in small signal stability. It contributes in the design consideration and the prediction of stability margin of an MG system.

REFERENCES

Abdel-Rahim, N. & J.E.Quaicoe (1996). Small Signal Model and Analysis of Multiple Feedback Control Scheme for Three Phase Voltage Source UPS Inverter. *Proceedings of Power Electronics Specialists Conference*, Baveno, Italy. 188-194.

Erickson, R. W. & Maksimovic, D. (2001). *Fundamental of Power Electronics Second Edition,* University of Colorado Boulder, Colorado, Kluwer Academic Publisher.

Justo, J. J., Mwasilu, F., Lee, J., & Jung, J.W. (2013). AC-Microgrids versus DC-Microgrids with Distributed Energy Resources: A review. *Renewable and Sustainable Energy Reviews,* 24, 387-405.

Katiraei, F., Iravani, M. R. & Lehn, P. W. (2007). Small Signal Dynamic Model of A Microgrid Including Conventional and Electronically Interfaced Distributed Resources. *IET Generation Transmission & Distribution,* 1**,** 369-378.

Krause, P. C., Wasynczuk, O. & Sudhoff, S. D. (2002). *Analysis of Electric Machinery and Drive System* Wiley-Interscience.

Kroutikova, N., Hernandez-Aramburo, C. A. & Green, T. C. (2007). State-space Model of Grid-Connected Inverters under Current Control Mode. *IET Electric Power Applications,* 1**,** 329-338.

Majumder, R. (2013). Some Aspects of Stability in Microgrids. *IEEE Transactions on Power Systems,* 28**,** 3243-3252.

Nimpitiwan, N. & Kaitwanidvilai, S. (2012). Static Output Feedback Robust Loop Shaping Control for Grid Conncected Inverter using Genetic Algorithms. *International Journal of Innovative Computing, Information and Control,* 8**,** 6081-6093

Pogaku, N., Prodanovic, M. & Green, T. C. (2007). Modeling, Analysis and Testing of Autonomous Operation of An Inverter Based Microgrid. *IEEE Transactions on Power Electronics,* 22**,** 613-625.

Tang, X. S., Deng, W. & Qi, Z. P. (2014). Investigation of the Dynamic Stability of Microgrid. *IEEE Transactions on Power Systems,* 29**,** 698-706.

Ugalde-Loo, C. E. & Ekanayake, J. B. (2010). State-Space Modelling of Variable-Speed Wind Turbines: A Systematic Approach. *IEEE ICSET.* Kandy, Sri Lanka.

Ugalde-Loo, C. E., Janaka B. Ekanayake & Jenkins, N. (2013). State-Space Modeling of Wind Turbine Generators for Power System Studies. *IEEE Transaction on Industry Application,* 48**,** 10.

Wu, R., Dewan, S. B. & Slemon, G. R. (1990). A PWM AC to DC Converter with Fixed Switching Frequency. *IEEE Transactions on Industry Applications,* 26**,** 880-885.